Bull. Mater. Sci. (2018) 41:70
https://doi.org/10.1007/s12034-018-1596-0

Rectifying resistance-switching behaviour of Ag/SBTO/STMO/p$^+$-Si heterostructure films

WENBO ZHANG, HUA WANG*, JIWEN XU, GUOBAO LIU, HANG XIE and LING YANG
School of Materials Science and Engineering, Guilin University of Electronic Technology, Guilin 541004, People's Republic of China
*Author for correspondence (wh65@guet.edu.cn)

MS received 29 June 2017; accepted 15 October 2017; published online 17 May 2018

Abstract. The $Sr_{0.88}Bi_{0.12}TiO_3/SrTi_{0.92}Mg_{0.08}O_3$ (SBTO/STMO) heterostructure films were prepared on p$^+$-Si substrates by sol–gel spin-coating technique, and the films had good crystallinity and uniform grain distribution. The heterostructure films with a structure of Ag/SBTO/STMO/p$^+$-Si exhibited a bipolar, remarkable resistance-switching characteristic, and $R_{HRS}/R_{LRS} \sim 10^4$. More importantly, the heterostructure films showed rectifying characteristic in the low resistance state (LRS), and the rectification ratio can reach 10^2 at ± 1 V. The dominant resistive-switching conduction mechanism of high resistance state (HRS) was Ohmic behaviour, and the LRS changed to space charge-limited current (SCLC).

Keywords. Resistive switching; heterostructure; $SrTi_{0.92}Mg_{0.08}O_3$; $Sr_{0.88}Bi_{0.12}TiO_3$; sol–gel.

1. Introduction

Resistive random access memory (RRAM), which has low energy consumption, simple structure, fast read–write speed, stable storage, information remained stable and compatible with COMS technology, was widely concerned around the world for the next-generation non-volatile memory in recent years [1,2]. The basic structure of RRAM cell is the sandwich structure with metal–insulator–metal (M–I–M) layers, and the M–I–M sandwich structure is so simple that can be structured with the highest maximum integration ($4F^2$) in theory [3], but this structure has serious problem of cross-talk after unit integration, one of the ways to solve this matter is to explore resistive-switching materials or devices that have self-rectifying effects [4]. However, there are fewer materials with self-rectifying characteristics, and which do not have good performance and stability [5,6]. So, the self-rectifying effects can be obtained by constructing diode with metal–semiconductor junction (Schottky barrier), homogeneous or heterogeneous pn junction [7]. In recent years, it was reported that the resistive-switching behaviour was found in $SrTiO_3$ [8] and Fe-doped $SrTiO_3$ films [9], which shows bipolar resistive switching. The Al/Cr–$SrTiO_3$/Si devices show self-rectifying property [10]. However, to the best of our knowledge, the self-rectifying characteristic based on the pn junction of $SrTiO_3$ system lacks investigation.

In this work, the pn heterojunction was constructed by combining p-type $SrTi_{0.92}Mg_{0.08}O_3$ (STMO) and n-type $Sr_{0.88}Bi_{0.12}TiO_3$ (SBTO) films. The resistive switching with self-rectifying effect was observed, and the origination of the self-rectifying effect in the Ag/SBTO/STMO/p$^+$-Si memory device was also clarified.

2. Experimental

The $Sr_{0.88}Bi_{0.12}TiO_3/SrTi_{0.92}Mg_{0.08}O_3$ (SBTO/STMO) films were fabricated on p$^+$-Si substrates by sol–gel spin-coating technique. STMO solutions were synthesized by using $C_{16}H_{36}O_4Ti$, $C_4H_6Sr \cdot 1/2H_2O$ and $Mg(CH_3COOH) \cdot 4H_2O$ as raw materials, acetic acid and $CH_3OCH_2COCH_3$ were used as solvent, and acetylacetone was used as chelating agents. $Sr_{0.88}Bi_{0.12}TiO_3$ solutions were synthesized by $C_{16}H_{36}O_4Ti$, $C_4H_6Sr \cdot 1/2H_2O$ and $Bi(NO_3) \cdot 5H_2O$, which is same as the STMO process. To obtain the heterostructures, the STMO thin films were first prepared on the (100)-oriented p$^+$-Si substrates by spin-coating the homogeneous solution at 4000 rpm for 30 s, followed by preheating at 120°C for 5 min and then, at 400°C for 10 min. Next, the SBTO films were deposited on the STMO layer by the same spin-coating process. The above processes were repeated three times. Finally, the heterostructures were annealed at 850°C for 10 min using rapid thermal annealing (RTA) technology at air ambient. The top Ag electrodes were deposited by thermal evaporation method with a metal shadow mask forming a test structure of Ag/SBTO/STMO/p$^+$-Si.

The crystalline phases of the SBTO/STMO films were characterized by X-ray diffraction (XRD, AXS D8-ADVANCE, Brucker). The surface morphologies were observed by scanning electron microscope (SEM, Hitachi S4800). The current–voltage (I–V) curves of heterostructure films with an

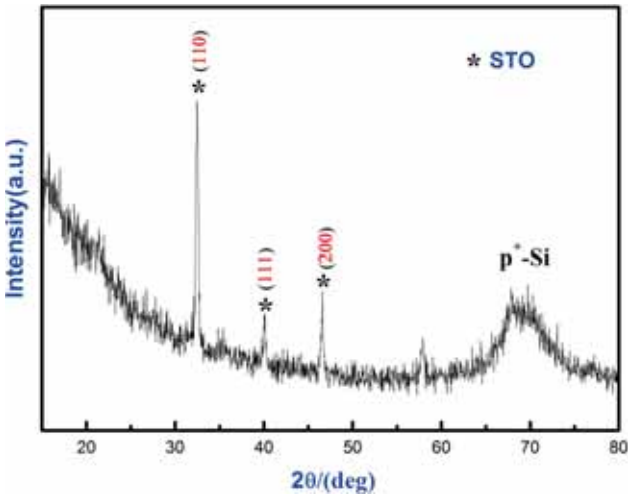

Figure 1. XRD spectrum of SBTO/STMO films on p^+-Si.

Ag/SBTO/STMO/p^+-Si structure were obtained at room temperature by Keithley 2400 source meter.

3. Results and discussion

XRD pattern of the SBTO/STMO heterostructure films on p^+-Si is shown in figure 1, the thin film growing on p^+-Si (100) substrate is polycrystalline structure and has a high degree of crystallinity. The main diffraction peaks of the heterogeneous films are fundamentally same as pure $SrTiO_3$ and the main diffraction peaks (110) and (200) of $SrTiO_3$ are evident. It can also be observed that the XRD pattern shows weak diffraction peaks originating from p^+-Si substrate.

Figure 2 is the typical SEM images of surface and cross-section morphologies of the SBTO/STMO films on p^+-Si. As shown in figure 2a, the top SBTO layer has good crystallinity and uniform grain distribution. The particle size of top SBTO layer is about 80 nm. Figure 2b shows that the thickness of the SBTO/STMO double layers is about 198 nm after spun-coating six layers, and there is no obvious interface between SBTO and STMO layers. Because the trace dopants in the SBTO and STMO films cannot cause lattice mismatch between SBTO and STMO layers, therefore, the SBTO film can grow on the bottom of STMO film. In addition, the SBTO/STMO layers combine tightly with the p^+-Si substrate.

The measurement illustration of the resistive-switching properties is shown in figure 3a. Figure 3b shows the resistive-switching characteristic of the heterostructure films with an Ag/SBTO/STMO/p^+-Si structure by I–V measurement. The sweeping voltage is in the sequence of $0 \rightarrow 8\,\text{V} \rightarrow -8\,\text{V} \rightarrow 0$. The heterostructure films exhibit a bipolar, remarkable resistance-switching characteristic, and the resistance ratio ($R_{\text{HRS}}/R_{\text{LRS}}$) of the high resistance state (HRS) to the low resistance state (LRS) is $\sim 10^4$. It is worth noting that the

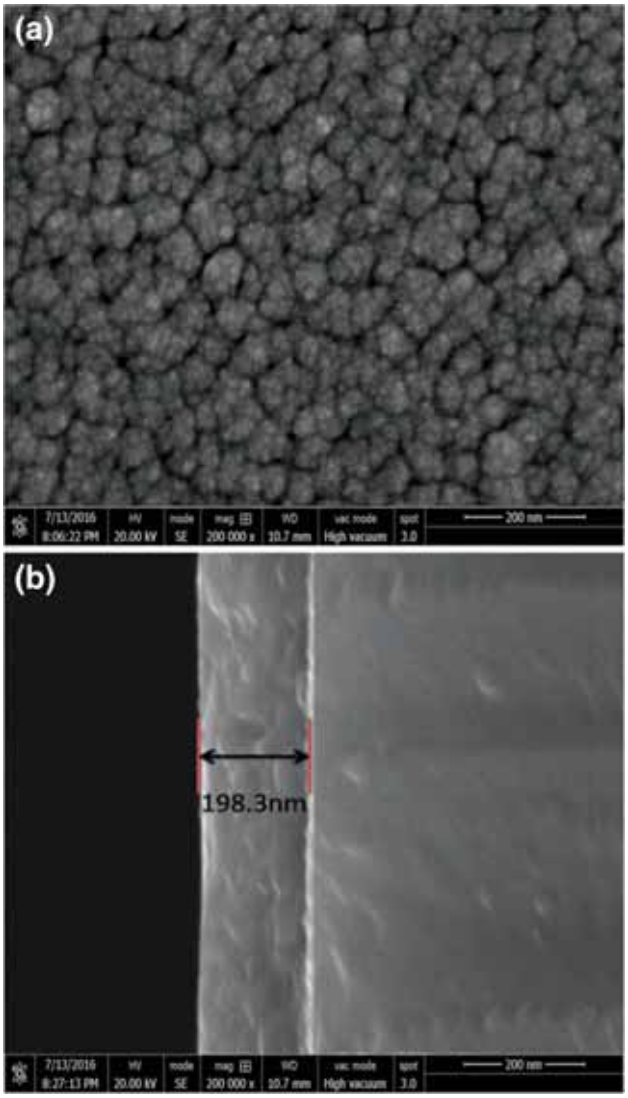

Figure 2. The surface morphology and cross-section morphologies of SBTO/STMO films on p^+-Si.

I–V curve of the heterostructure films is asymmetric LRS as shown in figure 3b. The device at the LRS shows a much higher current level at a positive bias compared to a negative bias. That is to say, the device at the LRS behaves as a diode, providing a rectifying ratio of 10^2 at ± 1 V, which indicates that the heterostructure films show a rectifier effect in LRS. The rectifying behaviour is beneficial for the elimination of the cross-talk in the cross-bar structure, and thus, misreading can be avoided [11]. The self-rectifying phenomena were previously observed in ZnO and HfO_2 films, both sandwiched by metal electrode (Al, Ni) and a Si electrode, which attribute to Schottky barrier [12,13]. However, in this work, this rectifying feature derives from the p-STMO/n-SBTO heterojunction.

To estimate the conduction mechanism of the Ag/SBTO/STMO/p^+-Si device, the $\ln|I|$–$\ln|V|$ scale curves of the I–V curve for the positive and negative biases are shown

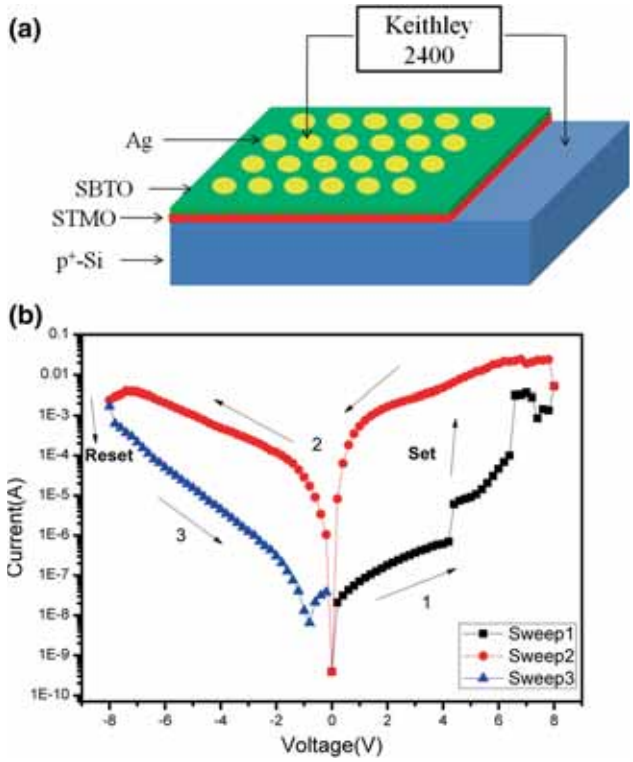

Figure 3. (**a**) The measurement illustration of resistive-switching properties and (**b**) resistive-switching characteristics of Ag/SBTO/STMO/p^+-Si.

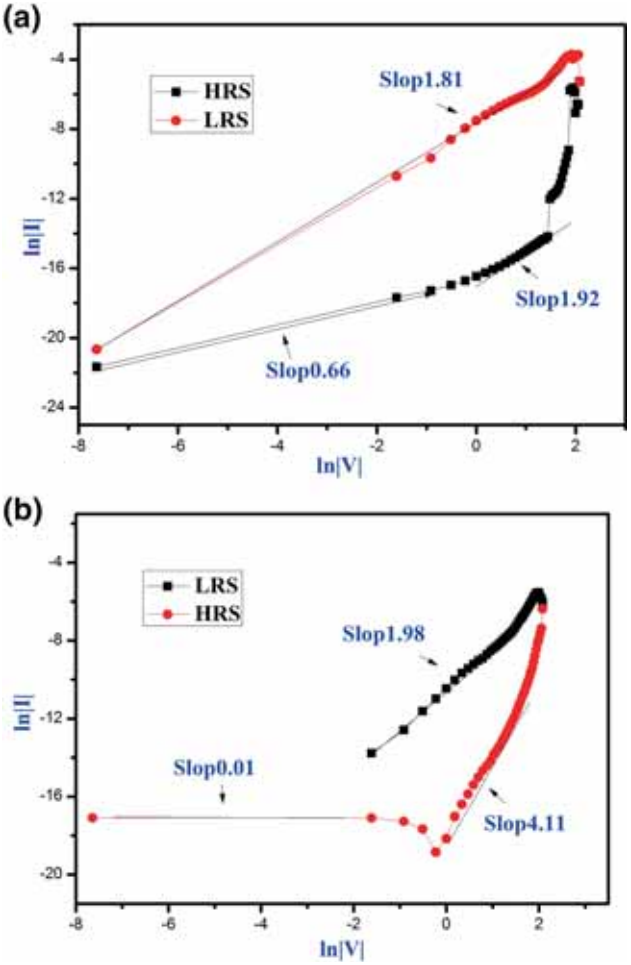

Figure 4. ln|I|–ln|V| scale curves of Ag/SBTO/STMO/p^+-Si: (**a**) positive and (**b**) negative biases.

in figure 4a and b, respectively. As shown in figure 4a, the I–V characteristic shows ohmic behaviour at low electric field for HRS (slope $\approx$ 1). However, at high external electric field, the slope increases to about 2, which conforms to the space charge-limited current (SCLC) mode, because the density of thermally generated free carriers in the films is predominant over the injected charge carriers, the current of the Ag/SBTO/STMO/p^+-Si device depends on the applied voltage and the conductivity of films. With the increase in external voltage, the carriers hop into the traps, and the excess electrons are trapped. This results in space charge [14]. When the resistance state changes back to the LRS, the slope is still approximately equal to 2. The conduction mechanism of Ag/SBTO/STMO/p^+-Si device can also be explained by SCLC mode. In figure 4b, under the negative bias, the slope of the I–V curve is still ~2 at HRS. When the carriers were fully released, the current of the device will be minimum, which indicates that the Ag/SBTO/STMO/p^+-Si device has the capacitance's hysteresis [15].

The mechanisms of the two resistive-switching types can be interpreted by oxygen vacancy [16,17]. As per filamentary resistive switching, high external electric field would create the filaments of oxygen vacancies through the whole multilayer. Therefore, after the electroforming-like soft breakdown process, it follows ohmic conduction at LRS. It is a typical bipolar resistive-switching behaviour that reverses migration of oxygen vacancies out of the filament, breaks the current path and returns the multilayer to HRS under negative bias. As a result, it exhibits a counter-clockwise polarity. The switching mechanisms originating from oxygen vacancy were also observed in the Al/n-ZnO/p-NiO/ITO memory devices [18].

Figure 5 demonstrates the resistance evolution of the HRS and the LRS of Ag/SBTO/STMO/p^+-Si device within 10^3 successive switching cycles. The results show that the resistance of the memory device at the LRS is stable during cycle test, and the resistance at the HRS shows slight fluctuation during the initial test stage, which means that the Ag/SBTO/STMO/p^+-Si device has better endurance characteristics.

The distribution of set voltage (V_{set}) and reset voltage (V_{reset}) is an important feature of RRAM, which would affect the stablity of writing and erasing data for RRAM devices. The distributions of V_{set} and V_{reset} of Ag/SBTO/STMO/p^+-Si device are shown in figure 6. From figure 6, it can be seen that the ranges of the set and reset voltages are 3 to 7 V and −5 to −7.5 V, respectively. The distribution of V_{set} is scattered, because the interface state of the heterojunction is not stable,

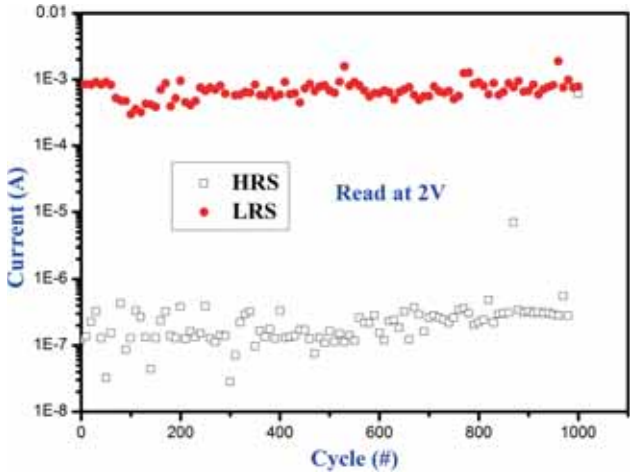

Figure 5. The reading endurance and stability of Ag/SBTO/STMO/p^+-Si.

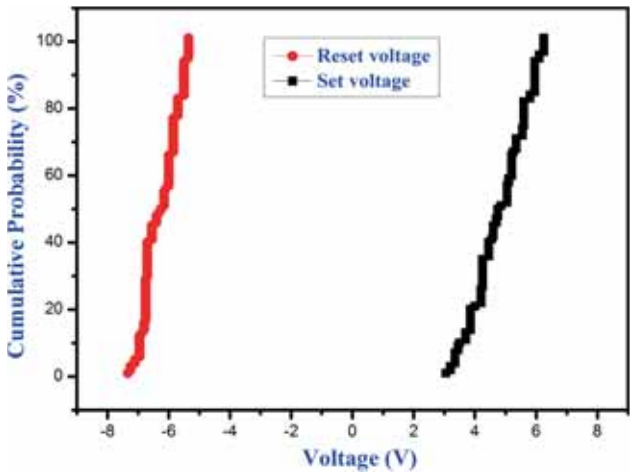

Figure 6. V_{set} and V_{reset} distribution of Ag/SBTO/STMO/p^+-Si.

it needs to be improved in follow-up studies. Furthermore, the distribution of the reset voltage shows a little concentration in the range of −5 to −7.5 V. The work voltage of integrated circuit is usually <5 V. However, the reset voltages in this work are >5 V, which cannot meet the demand of integrated circuit. The set and reset voltages are dependent on film thickness. The set and reset voltages can be decreased by reducing film thickness [19].

4. Conclusions

The SBTO/STMO heterostructure films were fabricated on p^+-Si substrates by sol–gel spin-coating technique, and the film has good crystallinity and uniform grain distribution. The Ag/SBTO/STMO/p^+-Si memory device exhibits remarkable bipolar resistance-switching characteristic, and its R_{HRS}/R_{LRS} is about 10^4. The devices show self-rectifying characteristic at LRS, and its rectification ratio reaches 10^2 at ±1 V. The Ohmic behaviour dominates the resistive-switching conduction mechanisms at HRS, and the SCLC acts on the LRS. Under 1000 cycle test, the device shows stable high- and low-resistances. The set and reset voltages have centralized values, but its value exceeds the standard voltage of 5 V. The self-rectifying property of the Ag/SBTO/STMO/p^+-Si RRAM can inhibit the cross-talk problem.

Acknowledgements

This work was supported by the Guangxi Nature Science Foundations, China (grant no. 2015GXNSFAA139253).

References

[1] Pan F, Gao S, Chen C, Song C and Zeng F 2014 *Mater. Sci. Eng. R-Rep.* **83** 1
[2] Linn E, Rosezin R, Kügeler C and Waser R 2010 *Nat. Mater.* **9** 403
[3] Chiu F, Li P and Chang W 2012 *Nanoscale Res. Lett.* **7** 178
[4] Lu H B, Yang G Z, Chen Z H, Dai S Y, Zhou Y L, Jin K J *et al* 2004 *Appl. Phys. Lett.* **84** 5007
[5] Cheng C H, Chou K I, Zheng Z W and Hsu H H 2014 *Curr. Appl. Phys.* **14** 139
[6] Ohta H, Hirano M, Nakahara K, Maruta H, Tanabe T, Kamiya M *et al* 2003 *Appl. Phys. Lett.* **83** 1029
[7] Zhang K, Long S, Liu Q, Lu H, Li Y, Wang Y *et al* 2011 *Sci. China* **54** 811
[8] Szot K, Dittmann R, Speier W and Waser R 2007 *Phys. Status Solidi-R* **1** R86
[9] Ruth M, Tobias M, Regina D and Rainer W 2010 *Adv. Mater.* **22** 4819
[10] Min Y S, Yujeong S, Yeon S K, Hee D K, Ho-Myoung A, Bae H P *et al* 2012 *Appl. Phys. Express* **5** 091202
[11] Zhang K W, Long S B, Liu Q, Lü H B, Li Y T, Wang Y *et al* 2011 *Sci. China Technol. Sci.* **54** 811
[12] Chen C, Pan F, Wang Z S, Yang J and Zeng F 2012 *J. Appl. Phys.* **111** 013702
[13] Lu D, Zhao Y, Anh T X, Yu Y H, Huang D, Lin Y *et al* 2014 *IEEE Trans. Electr. Dev.* **61** 2294
[14] Ielmini D 2011 *IEEE Trans. Electr. Dev.* **58** 4309
[15] Xie Y W, Sun J R, Wang D J, Liang S and Shen B G 2006 *J. Appl. Phys.* **100** 033704
[16] Park J, Kwon D H, Park H, Jung C U and Kim M 2014 *Appl. Phys. Lett.* **105** 183103
[17] Tang Z, Xiong Y, Tang M, Cheng C, Xu D, Xiao Y *et al* 2014 *Jpn. J. Appl. Phys.* **53** 035503
[18] Lu H, Yuan X, Chen B, Gong C, Zeng H and Wei X 2017 *J. Sol–Gel Sci. Technol.* **82** 627
[19] Millaty M, Pilsun Y, Wei H, Bo W L and Chunli L 2015 *Nanoscale Res. Lett.* **10** 168